

Sandia National Laboratories
University Alliance Design Competition
MEMS Educational Design Category

Pressure-Sensitive Microvalve

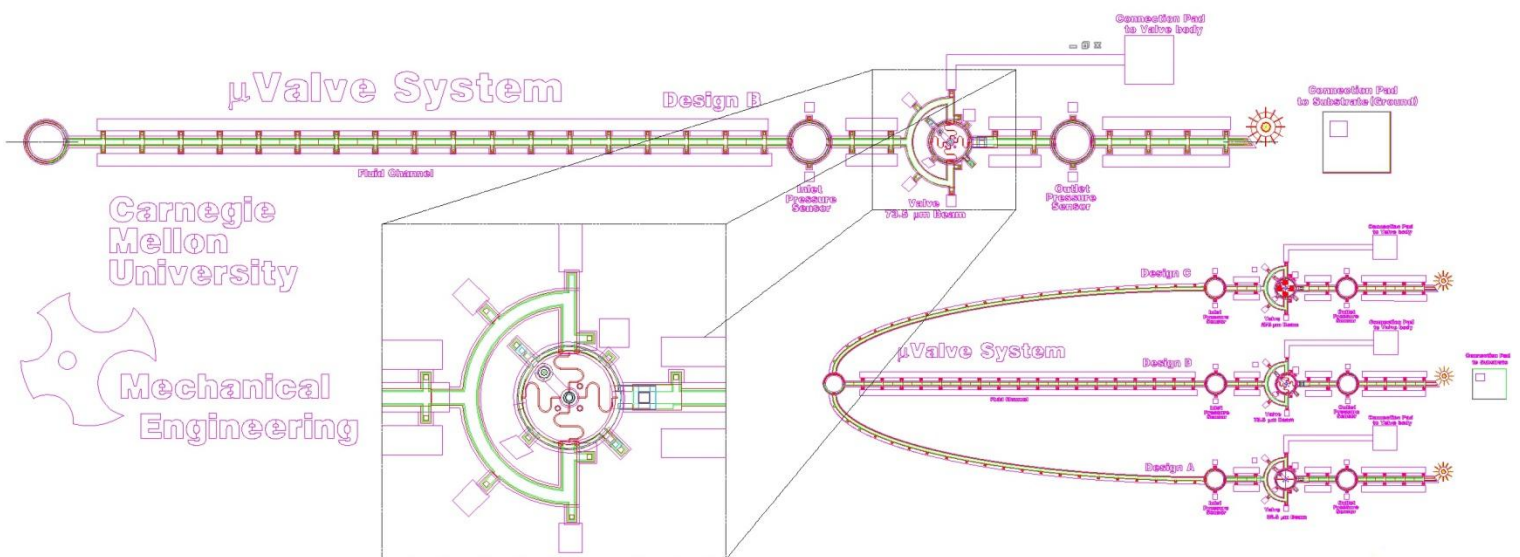
Vitali Brand (lead), Henry Kung, Sam Powers, Emreacan Soylemez
Department of Mechanical Engineering
Carnegie Mellon University

Faculty Advisor: Dr. Maarten de Boer

April 5, 2011



Mechanical Engineering
Carnegie Mellon University



Section 1: Abstract

Microvalves have proven to be a staple component in current MEMS technology and are extremely useful in explaining as well as illustrating complex concepts in the field of μ -engineering. This paper presents an innovative, fully-operational pressure-sensitive μ valve used for educational purposes to show control of fluid flowing on a wafer. The design is exceptionally versatile because it allows for precise control over both the pressure at which the valve opens and the pressure at which the valve closes by varying the valve-beam compliance over three designs. Several tests are outlined targeting undergraduate and graduate-level engineering students to illustrate the operation of μ sensors and μ valves and to introduce topics such as beam mechanics and electrostatic actuation. This valve design takes advantage of unique features in the SUMMiT V process by creating release channels through stacked etch holes, creating sub μ m gaps using dimple layers to enhance pressure control, and using a nitride cut to serve as an interconnect to actuate the electrode under the valve body. Additionally, a front-side-only plumbing strategy is employed so that no post-processing is required. These experiments will awaken student's awareness of the vast possibilities in MEMS.

Section 2: Introduction

For centuries, the preferred method of fluid flow control has been via valves; the most common categories being screw-based and switch-based. Screw-based valves, such as globe, bellows, and needle valves, require an external rotation of a handle to control a movable barrier to adjust flow. Alternatively, flow barriers in switch-based valves, such as spring-driven diaphragms, are moved by a set pressure. Although μ valves differ from macrovalves in fabrication and actuation, they typically involve a type of switch mechanism. Applications of mechanical diaphragm, ball, and flapper μ valves are seen in heart valve prostheses and piezoelectric pumps [1]. Although they consume higher power, thermally activated μ valves apply large closing forces and are perfect for applications where low leakage is instrumental [1]. Flapper valves actuated by electrostatic force have been created for gas flow regulation and are used in on/off switch μ valve control. Precise flow control is of utmost importance in the field of μ fluidics and this characteristic enables devices such as inkjet printers, drug-delivery systems, and artificial heart pumps [1-2]. Furthermore, many devices, such as gas analyzers, are more compact, sensitive, and precise by utilizing technologies in μ fluidics [3].

One of the most common types of μ valves is electrostatic, after which the design presented in this paper is modeled. Many current devices utilize electrostatic μ valves such as rarefied gas control systems [4-5], direct methanol fuel cells [6], nitrogen release components in microengines [7], and silicon micromachining for precise power control [8]. For applications where the response time is crucial, electrostatic μ valves have been developed with response times of under one millisecond [9]. Yobas *et al* introduced an electrostatic μ valve for the purpose of enabling a pneumatic refreshable Braille display system in which the μ valve is electrostatically closed against a differential pressure of 82.7kPa with an applied voltage of 68V [10-11].

For μ fluidic analysis, pressure sensors are popular tools used in conjunction with valves. While micro-Pirani sensors are well suited to measuring sub-atmospheric pressures [12], most sensors used to measure super-atmospheric pressure are made from deformable diaphragms [13]. These pressure sensors, which are easily created using the SUMMiT V process, are made from a cavity (usually circular) that is sealed by an elastic diaphragm. A pressure differential across the

diaphragm causes it to deflect so a larger sensor diameter is associated with greater sensitivity [14]. While both piezoresistive and capacitive sensors [15-19] have been used to measure the diaphragm deflections, interferometers are the preferred method since they do not require any additional processing on the diaphragm [20-23].

The μ valve proposed in this report is electrostatically driven to create a variable opening and closing pressure to regulate air flow. In addition, by using surface μ machining to produce these valves, they can be integrated into existing devices and control flow on the wafer [24]. Diaphragm pressure sensors are placed such that the pressure of the fluid entering and exiting the valve is monitored and another sensor is integrated with the valve to monitor whether the valve operates within the desired pressure range. The integrated sensor will also indicate the pressure of the fluid leaving the valve. These systems are connected together using long μ channels that are designed to be easily etchable. A gear is located at the exit of each system and will spin when the valve is open and will remain stationary otherwise.

2.1 Design Advantages

The proposed μ valve design is loosely based on the mechanical check valve in the micro-gas analyzer from Sandia National Labs [29] although there are profound differences. The advantages of this innovative design follow:

- External plumbing connections, using tubing sealed by semiconductor-grade epoxy, are accomplished from the top-side of the wafer. A backside (Bosch) etch is not required, and the design is fully compatible with the standard SUMMiT V process flow.
- The μ valve can easily be integrated as a component in a MEMS device because it releases fluid into a specific on-wafer flow circuit.
- The top of the valve simultaneously operates as a pressure sensor to indicate fluid flow.
- Etch holes allow for extra-long channels to be incorporated in the design without relying on non-standard etch time, and are readily sealed with epoxy (Section III – Test Setup).

This white paper describes the operation and functionality of the pressure-sensitive μ valve and outlines an educational plan for an undergraduate or graduate level MEMS class.

Section 3: Description

The overall design is shown in Figure 1 in Appendix A and consists of a valve orifice, μ channels, three pressure sensors (inlet, on top of the valve, and outlet), a μ valve, and a rotor-style flow indicator. The post-decimal digits in Figures 1.00-1.12 correspond to specified cross-sections labeled in Figure 1. On the module, there are two additional types of valves connected by the same valve system orifice as shown in Figure 1.13, with varying compliance of the valve beams. These three types are labeled designs A, B, and C with increasing compliance from A to C. The front-side-only plumbing strategy as described in the *Test Setup* section and in Figure 2. This section discusses Design B in detail.

3.1 Surface Micromachine Design and Components

The gas enters the valve system through an orifice (called the “valve system orifice”) as shown in Figures 1.00 and 1.01. The gas then travels through a μ channel shown in Figures 1, 1.02 and 1.03 to the inlet pressure sensor (Figures 1.04 and 1.05). This pressure sensor has a

diaphragm that deflects relative to the pressure differential across it as measured by interferometry. The deflection can be related to pressure using equation 1 described in the modeling section. Most features in the design have etch holes that ensure that the release process occurs properly. Those holes are sealed as will be described in the *Test Setup* section.

Upon exiting the pressure sensor, the gas travels through a μ channel that splits into two directing the flow into the valve from opposite entrance points (Figure 1.06). This allows a more balanced and uniform pressurization of the valve. As the pressure accumulates in the lowest level of the valve, the only barrier between that level and the valve exit channel is the valve body as shown in Figures 1.06 through 1.09. In these images, the valve body is in the center and appears to be out of contact with the rest of the structure, however, it is held in place using ‘S’ shaped beams that are connected to the walls of the valve. Those “S” beam cross-sections appear intermittently in Figures 1.06 and 1.09.

Electrostatic force that is applied to the valve body holds it shut. This prevents gas from passing through the valve until the force on the valve body due to gas pressure exceeds a desired limit. This limit can be adjusted by changing the electrostatic pressure between the MMPOLY0 actuation pad and the valve body. The entire valve assembly is electrically grounded. To apply the electrostatic force, the MMPOLY0 actuation pad is connected to the substrate through a hole in the nitride. The voltage bias is applied to the system by placing an electrical probe on the pad that contacts the substrate (shown in Figure 1.12) and grounding any MMPOLY0 layer that is in contact with the valve system.

Once the gas pressure is high enough to push the valve body upwards (i.e. open the valve), gas passes through the valve. However, if the gas pressure is higher than the desired pressure level, the valve body (made from MMPOLY12) is designed to stop the flow because it is pressed against the inner valve exit orifice (made from MMPOLY3) as can be seen in Figures 1.06 through 1.09. The upper pressure bound has a strong dependence on the compliance of the valve beams that hold the valve body. A theoretical and computational analysis of the valve behavior is discussed in the modeling section and Appendix E.

Other features of the valve include pillars (Figure 1.07) which hold in place the layers between which the valve body moves. These pillars are important since the valve body can exert substantial stresses on bounding layers. The valve has a variety of etch holes on its sides, including the multi-layer etch holes (Figure 1.08) that aid with the removal of the sacrificial oxide layers during the release step. The upper most layer of the valve, which is not connected to any pillars, acts as a diaphragm pressure sensor.

Gas exits the valve through a bridge shown in Figure 1.09, entering a μ channel that leads it to the outlet pressure sensor which monitors the gas pressure just prior to its exit from the valve system. Next, the gas flows through the final μ channel which is aimed at a rotor that spins (Figures 1.10 and 1.11) if the flow is strong enough and the valve is open. It is possible to connect this to another gear to generate power or drive a system.

3.2 Test setup

The MEMS pressure valve is connected to an air supply through a system of tubes and connectors with the end of the smallest tube in the system bonded to the valve system orifice using semiconductor grade epoxy (see Figure 2 in Appendix B for a diagram of the entire external system setup). This tube is bonded perpendicularly to the wafer such that the outer diameter of the valve orifice is inside the inner diameter of the tube, ensuring that the fluid will enter the orifice from the tube. Considering that the orifice is 90 μ m in diameter, it is a delicate

task to place the tube above it such that there is a passage for the fluid into the orifice. Therefore, a tube with a comparatively large diameter of 795 μm (1/32") and a microscope with low magnification are used to simplify aligning the tube.

A gas cylinder containing nitrogen is used in conjunction with a pressure regulator to allow for the precise control of the system pressure. The regulator and bellows valve (Figure 2, Appendix B) output to a standard 1/4" Swagelok fitting allowing 1/4" tubing (Teflon IDxOD 0.19"x0.25") to be connected to it. An appropriate tube reducer is used to connect the 1/4" tubing to the 1/32" tubing (Teflon IDxOD 0.013"x0.03"). These plumbing materials are available through Scientific Commodities. Teflon is chosen as the tubing material because it is soft enough to avoid crushing the μ channels.

Semiconductor grade brittle epoxy (EPO-TEK 353ND), which is designed to bond materials such as plastics and silicon, is used to bond the 1/32" tubing to the valve orifice on the wafer. The epoxy has two parts (designated: A and B) that need to be mixed in a ratio of 10:1 units of A:B for precipitation to initiate. The mixing can be done on a flat surface using a toothpick because the epoxy is very viscous (5000 times as viscous as water at 23⁰C). Epoxy is smeared onto the periphery of the tubing using a toothpick while being careful not to block the entrance. The tube is aligned to the marked annulus (Figure 1.13) using a microscope with a CCD camera and gently pressed against the orifice allowing the epoxy to seal any small gaps between the tube end and the wafer surface. The epoxy will not leak into the structure due to its high viscosity. Note that the orifice is connected to the valve through long μ channels allowing the user to epoxy the tube without accidentally smearing it over the valve or sensors. An exposure to 150°C will cure the epoxy within one minute which is accomplished using a heat gun (set to low power) - the Teflon tubing is heat-resistant at this temperature.

The most significant challenge is to use epoxy to seal the etch holes that are located roughly 10 μm away from the pressure sensors and the valve since the sensors are useless if they are exposed to the epoxy. A 10x magnification microscope is used to identify the etch holes close to the sensors and a micrometer-controlled needle is used to move small quantities of epoxy over the etch holes. There is no concern of the epoxy leaking into the etch holes and sealing the channels because the epoxy is very viscous. It is not necessary to be nearly as precise when sealing the etch holes farther from the sensors.

Once the tubing is connected and the etch holes are sealed, the valve is operational. Since the sensor's diaphragms are sensitive, make sure to not over-pressurize the system by only specifying pressure ranges below 300 kPa. The deflection of the diaphragms in the pressure sensors can be monitored using an interferometer setup and MEMScript software is used to convert the interferometric measurements into vertical deflection of the diaphragm [25].

3.3 Uniqueness

Although μ valves hold a key position in MEMS devices in general, no educational papers devoted to understanding the mechanics behind the operation of pressure-sensitive valves or μ valves have been developed [30-31]. This design intends to fill that gap. Although there are many existing techniques to manufacture pressure μ valves, the proposed design is substantially simplified because the SUMMiT V process enables the structure to be more compact. The valve itself not only contains a pressure sensor, but consists of four stacked channels with vertical gap sizes ranging from 0.3 μm to 2.0 μm . The 0.5 μm gap between the activation pad and the valve body allows for a higher operational pressure range. Because the maximum allowed etch length in the SUMMiT V process is 38 μm , etch holes, which are used to etch away oxide from inside

the structure during the release step, are incorporated to create long μ channels. These etch holes are later sealed with a semiconductor grade epoxy as discussed in the *Test Setup* section above. As specified previously, a distinctive feature of this model is the on-wafer flow through the valve. This is a valuable ability since it allows for integration of other on-wafer flow systems. This design presents a pioneering approach to μ fluidic education with real innovative applicational value.

3.4 SUMMiT-V's Specific Strengths

This design utilizes many aspects of the SUMMiT V process, including all MMPOLY layers, and can be used as an educational tool in understanding many MEMS fabrication and design techniques. For instance, in order to maximize the electrostatic force on the valve body, a dimple cut feature is used. This reduction in the gap size between the valve body and the activation pad from 2 μ m to 0.5 μ m enables a larger operational pressure range for this design. The flat topography produced through the SUMMiT V process allows the valve body to seal properly preventing leakage and such small gap sizes to be accurate. Stacked etch holes are used to release the inside of the multi-layered valve from the sacrificial oxide. This requires only one sealing procedure. When the fluid exits the valve and passes through the channel, it is blown out onto a rotor modified from a structure in the gear generator.

Section 4: Educational Value, Audience, and Lesson Plan

A μ valve can be a powerful way to demonstrate the vast possibilities of microfabrication. This device will show how a complex system can be designed with a relatively simple base procedure. This will hopefully inspire scientists and engineers to come up with practical devices that use similar concepts as well as encourage students to explore the world of MEMS. The educational tests outlined intend to show the following:

- A measurement method for pressure sensors
- Control of opening pressure due to electrostatic force
- Determination of the closing pressure both experimentally and theoretically
- An illustration of each valve's operational pressure range

4.1 Target Audience

Since the operation and fabrication of μ valves are better understood by an individual with some background in mechanical engineering, this device targets undergraduate and graduate engineering students with the purpose of introducing microfluidic devices. The educational outline described below could be used as a laboratory exercise in a MEMS or a mechanical design class. The intent of this design is to offer students a straight-forward device that provides a fundamental understanding of several important MEMS and microfluidics concepts.

4.2 Lesson Plan

To better understand the operation and functionality of the pressure-sensitive μ valve, several experimental procedures are presented to illustrate its capabilities and show the effect of specific design parameters with additional procedures and tests in Appendix F. In addition, a leak test is also outlined in Appendix F.

1) Pressure Sensors – Experimental Calibration

The first test will focus on the three sensors in the system – inlet, valve, and outlet. Adjust the interferometer and view so that all three pressure sensors in the valve assembly are visible in order for the pressure readings to be taken simultaneously. Set the air pressure to 40 kPa. Use the interferometer to record the deflections of all three sensors. Increase the pressure by 40kPa and retake the sensor readings. Continue until the pressure has reached 300 kPa. Use Figure 4 in Appendix D to convert the deflection measurements to pressure values and compare the three sensor readings. All three sensors should read approximately the same pressure at a specific input pressure. Reset the air tank to the nominal pressure.

2) Electrostatic Opening Pressure

This test illustrates the ability of this μ valve to remain closed up to a specific pressure when electrostatic pressure has been applied. Set the air tank pressure to 40 kPa and the voltage to 200 V. Use the interferometer to record the pressure readings of all nine sensors (three from each design). Continue this procedure, increasing the pressure by 40 kPa after each measurement, until 300 kPa is reached. Return the air tank pressure as well as the applied voltage to zero. The deflection data obtained is analyzed to determine the opening pressure of each valve given the specific applied voltage as discussed in Appendix F.

3) Closing Pressure

This valve has the important attribute that it seals shut when the pressure exceeds a certain value and this test explores that specific ability. Once the system is setup as in the previous section, set the air tank pressure to 40kPa with no voltage applied to the system. Take pressure readings of all nine sensors and increase the applied pressure as in the last two tests. Then, return the air tank pressure to zero. The deflection data obtained is analyzed to determine the closing pressure of the valve as discussed in Appendix F.

4) Variable Pressure Sensitive Control

This valve is extremely versatile since the electrostatic force can be used to control the opening pressure of the system resulting in many obtainable operational pressure ranges. A constant electrostatic force only controls the opening pressure since the force is very weak when the valve is closed-up (see Figure 4, gap of 2.5 μ m). For this procedure, only the design B will be considered. Once the system is setup as in the previous tests, set the air pressure to 40 kPa and the applied voltage to 100 V. Take the pressure readings and increase the pressure as in the previous tests. Then, return the air tank pressure as well as the voltage to

Section 5: Modeling

The purpose of this analysis is to gain insight into the mechanical behavior of the various components of the μ valve design. Specifically, the deflection of the valve beams holding the valve body due to electrostatic force and the fluid pressure is modeled. The deflection of the diaphragm pressure sensors as a function of pressure is also presented.

According to Bernoulli's equation, the large decrease in cross sectional area of the flow channels occurring as the fluid enters the microstructure from the tubing, causes a large

reduction in fluid pressure. When the valve is closed down, the fluid fills the chambers prior to the valve and the shock due to the initial fluid contact is negligible. At this point, the only pressure that the valve body experiences (besides the electrostatic component) is due to the pressure gradient across the boundary. Once the valve is open, there is an interplay of several affects which are the electrostatic force on the membrane, the force exerted by the fluid flow, and the receding pressure gradient across the valve body. If the contributions from flow rate and pressure begin to dominate relative to the electrostatic force and the elastic reaction forces from the beams, then the valve will close. The relationship between the pressure membrane deflection ($\delta_{diaphragm}$) and the pressure in the sensor (P) are expanded from an analysis done by Timoshenko et al [26] as follows:

$$P = \frac{16Et^3\delta_{diaphragm}}{3R^4(1-\nu^2)} \quad (eqn 1)$$

The definition and value of these variables are found in Table 1 in Appendix C while a logarithmic plot of this relationship for this specific system is found in Figure 4 in Appendix D. By measuring the deflection of the membrane with an interferometer, the pressure can be found using Figure 4.

In order to close the valve initially, the electrostatic force must be large enough to overcome the elastic force of the valve beams. The pressure on the valve body that results from the electrostatic force (P_{elec}) is defined as:

$$P_{elec} = \frac{\epsilon_0}{2} \left(\frac{V}{g+x} \right)^2 \quad (eqn 2)$$

The definitions and values of these variables are found in Table 1 in Appendix C while a brief analysis of this force is found in Appendix D. To determine the elastic force, the valve body and valve beams are considered to be fixed-fixed beams with an applied center load. In this analysis, both the theoretical beam deflections using equations 4 and 5 and an FEM model were analyzed and compared (Appendix E). The theoretical beam deflections agreed closely with the FEM model for designs A and B, but differed dramatically in design C as seen in Figures 6-8. This difference is due to the curved geometry of the beams in design C which are not accounted for in the theoretical approach. Once the deflection (δ) and electrostatic force on the valve body are known as well as the pressure of the flow (P_{flow}), the effective spring constant (k_{eff}) of the valve beams can be found by equation 3:

$$k_{eff} = \frac{\pi D_e^2 P_{elec} - \pi D^2 P_{flow}}{4\delta} \quad (eqn 3)$$

Section 6: Summary

Microvalves have a myriad of useful current applications and a large potential in future microfluidic design. The device proposed in this paper is not only an informative demonstration of the capabilities of the SUMMiT V process, but also is a valuable educational tool. By going through the design and fabrication process, many intricacies of the SUMMiT V process can be discussed and practiced while working towards a usable device. In addition, the experiments discussed provide insight into the inner workings of μ valves and can be used to introduce complex topics in electrostatic actuation or in beam mechanics such as nonlinear fixed-fixed beams. In addition, the experiments are relatively simple to construct and do not need extensive measuring equipment to obtain the required results. This device will be instrumental in introducing or expanding on key concepts found in a MEMS class and encouraging student to explore this exciting field.

Appendix A: System Description – Surface Micromachine Design and Components

The layout image in Figure 1 is plotted by AutoCAD. The post-decimal digits in Figures 1.00-1.12 correspond to specified cross-sections labeled in Figure 1, i.e. Fig. 1.05 is a cross-section through “5” in Figure 1. Cross-section images were generated by Sandia MEMS Design Tools. The 3D images were generated by Sandia MEMS Design Tools as SAT files and then modified in SolidWorks (unless specified otherwise).

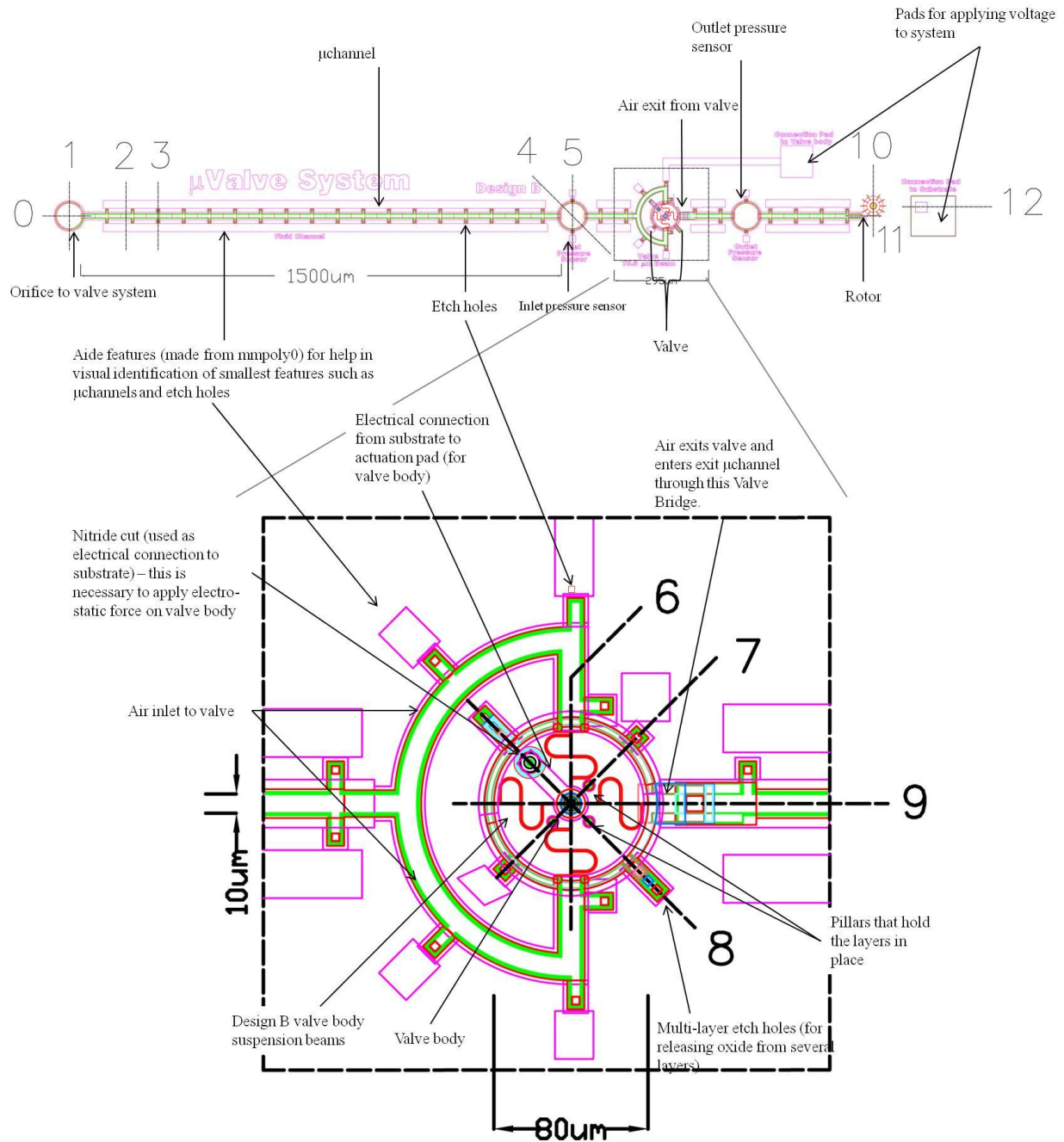


Figure 1: AutoCAD 2D layout of the pressure sensitive μ valve design. This view includes an orifice to the valve system, μ channels, inlet pressure sensor, μ valve, outlet pressure sensor, rotor and pads for applying voltage to the system. A detail of valve design B has been illustrated.

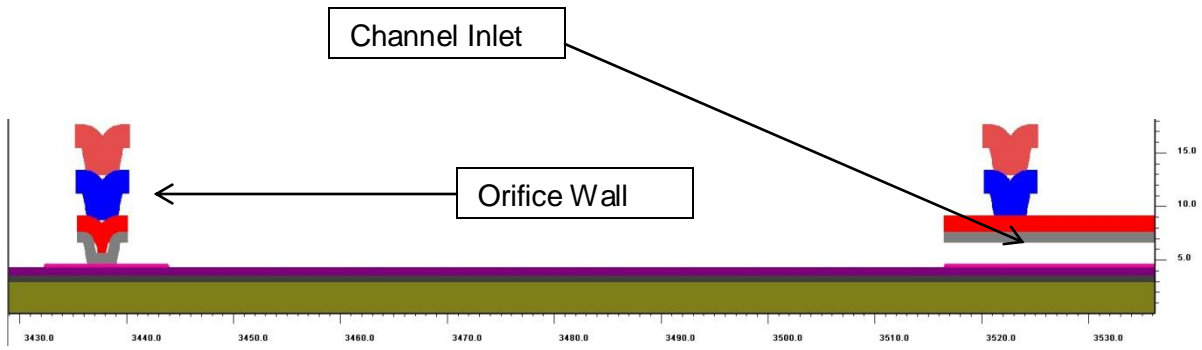


Figure 1.00: Cross-section model of the orifice. The orifice is the input flow source connecting to the μ channel on the right. The tube connection is described in Appendix B (Figure 2).

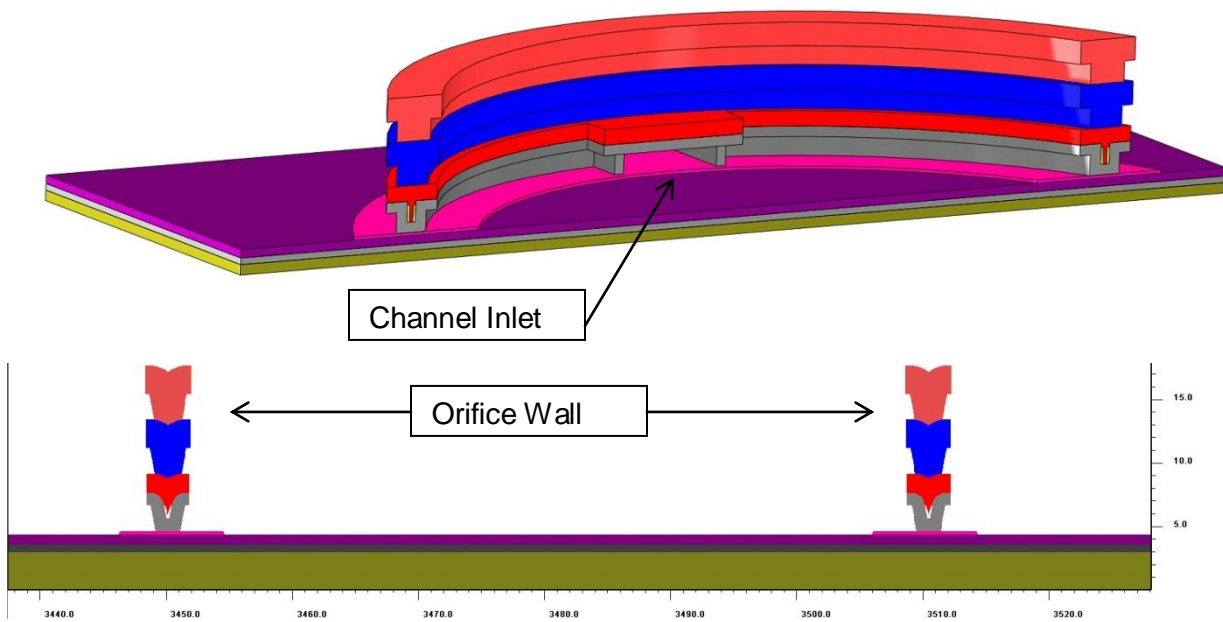


Figure 1.01: A 3D modeler cut view of the orifice and a cross-section view.

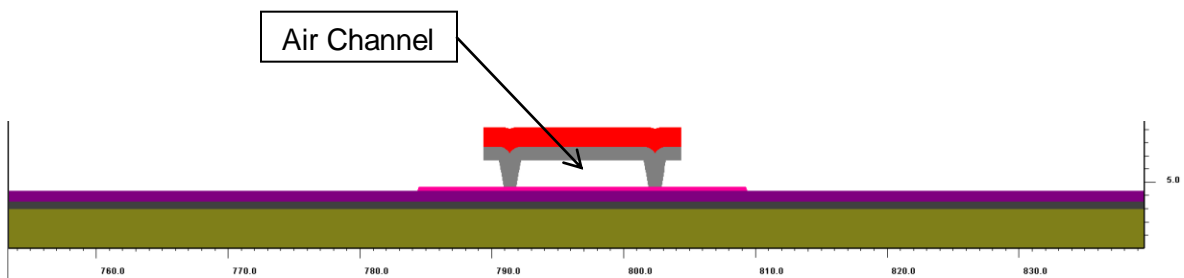


Figure 1.02: A cross-section view of the μ channel. MMPOLY1 and MMPOLY2 layers bound the channel on three sides and the MMPOLY0 layer on the fourth.

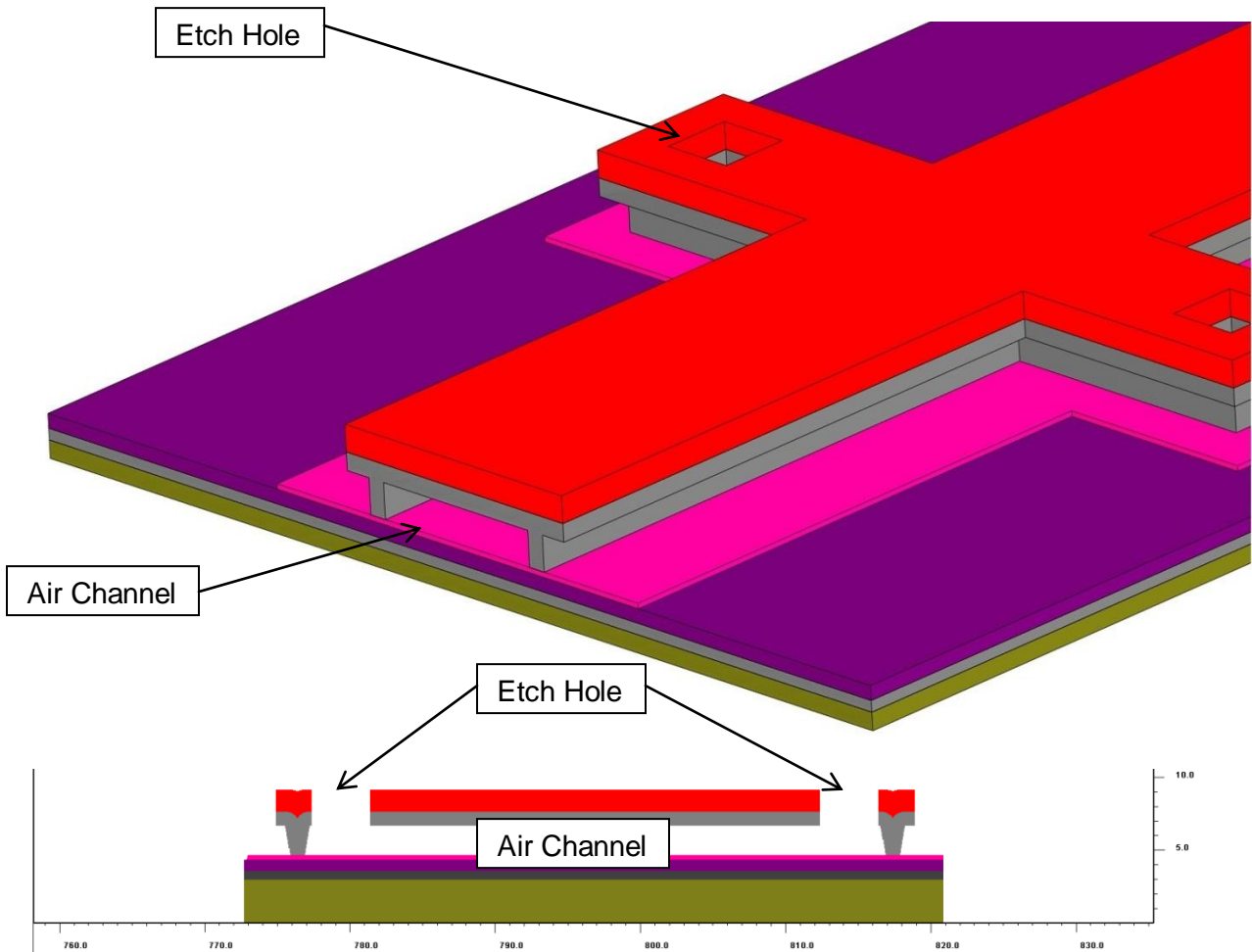


Figure 1.03: 3D modeler view and cross-section model of μ channel with etch holes. These etch holes make it possible to fabricate long channels without requiring post micromachining. Etch holes will be sealed as described in the *Test Section*.

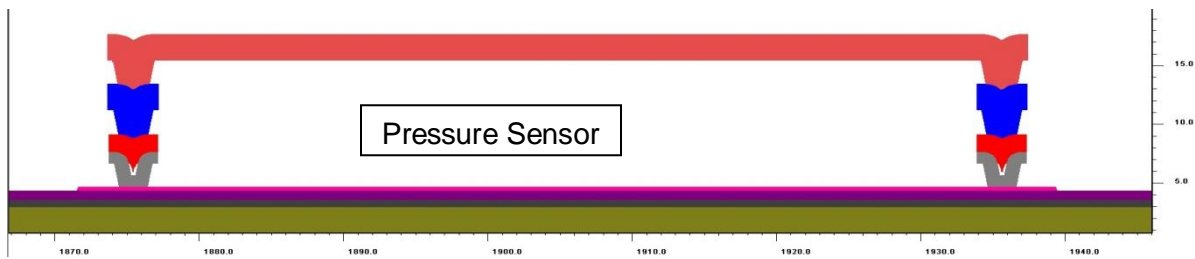


Figure 1.04: Cross-section model of diaphragm pressure sensor. Applied pressure deflects the diaphragm and interferometric deflection measurements indicate the pressure.

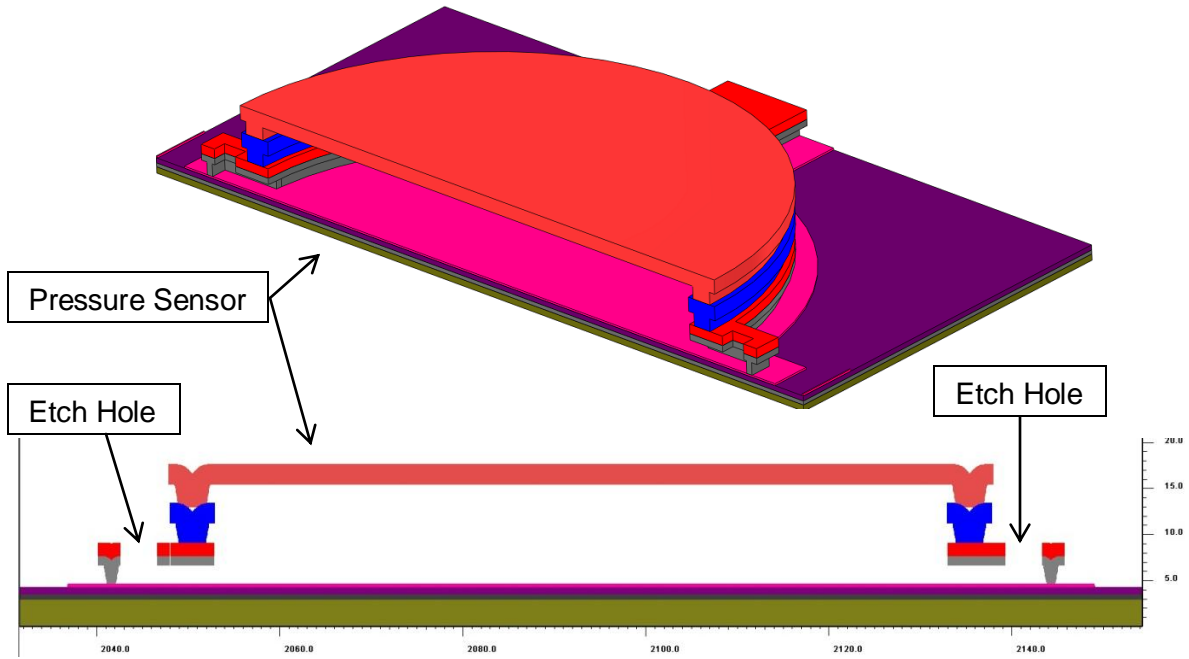


Figure 1.05: 3D modeler view and cross-section of diaphragm pressure sensor with etch holes. The etch holes enable full diaphragm release with the standard SUMMIT V process.

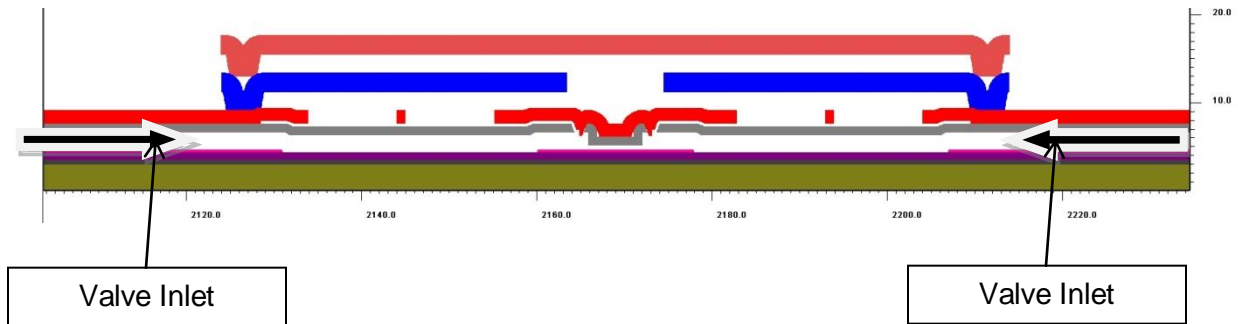


Figure 1.06: Cross-section model of pressure valve showing flow inlet to valve.

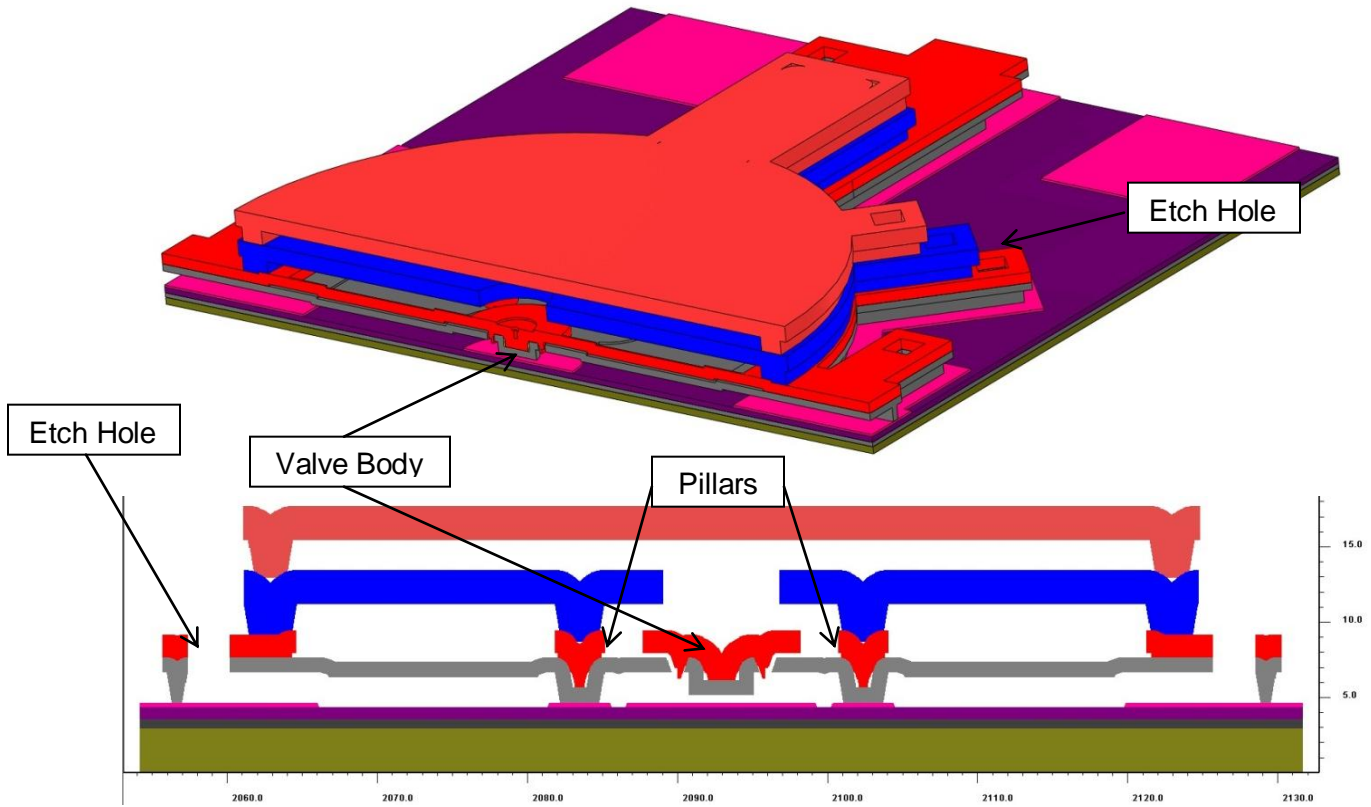


Figure 1.07: 3D modeler view and cross-section model of pressure valve showing pillars near valve body and etch holes on the sides.

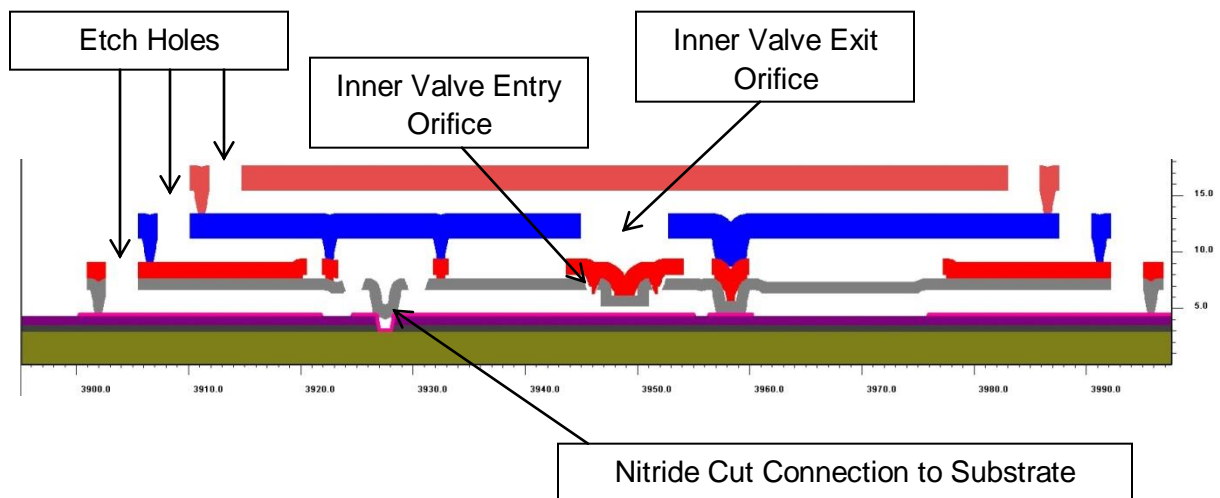


Figure 1.08: Cross-section model of pressure valve showing the nitride cut as well as the multilayer etch holes. The valve cannot contain release holes. Therefore, the multilayer etch holes enable each SacOx layer to be removed.

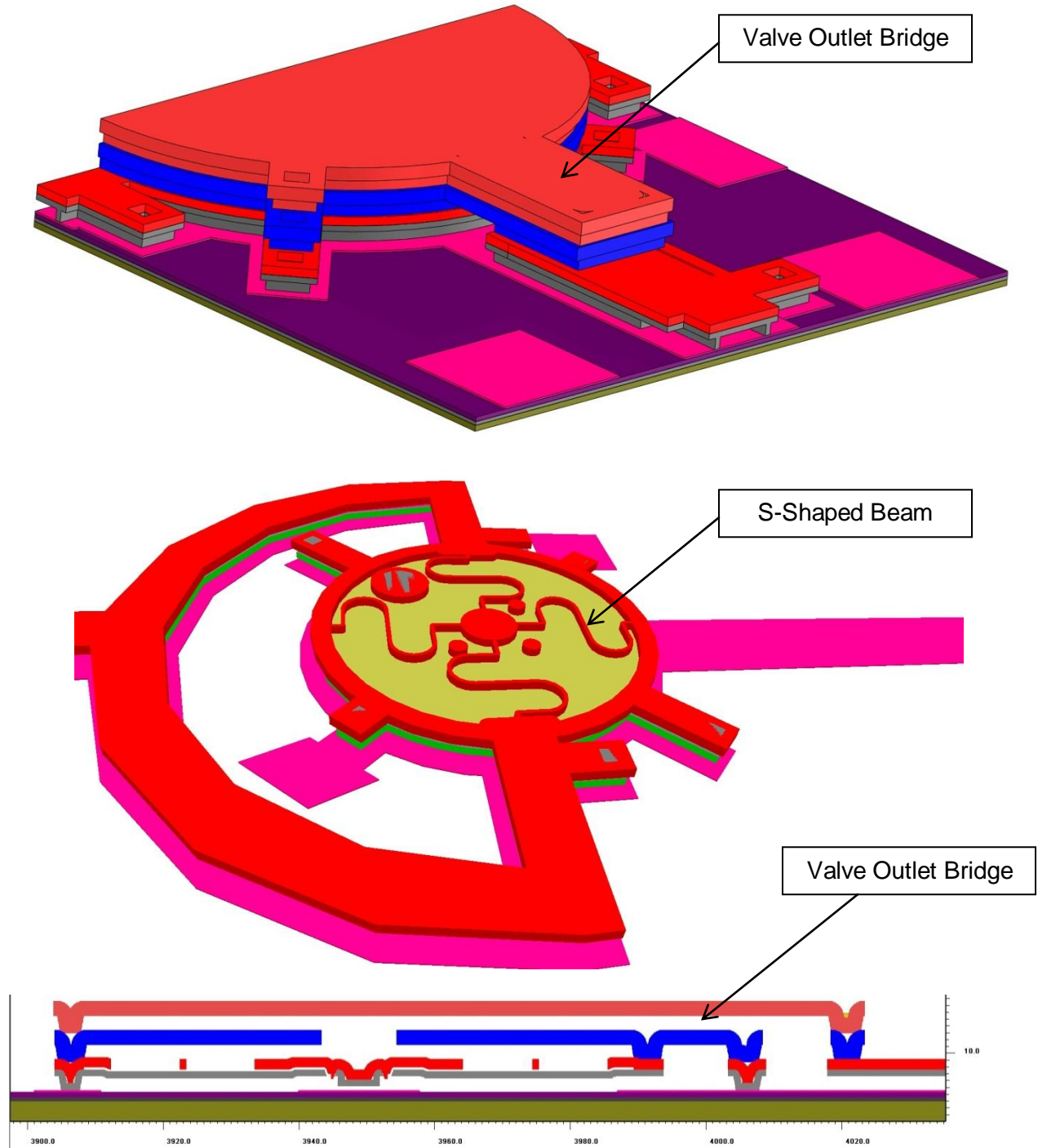


Figure 1.09: A 3D modeler and cross-section views of design B pressure valve. The S-shaped beams holding the valve body as well as the outlet channel are shown.

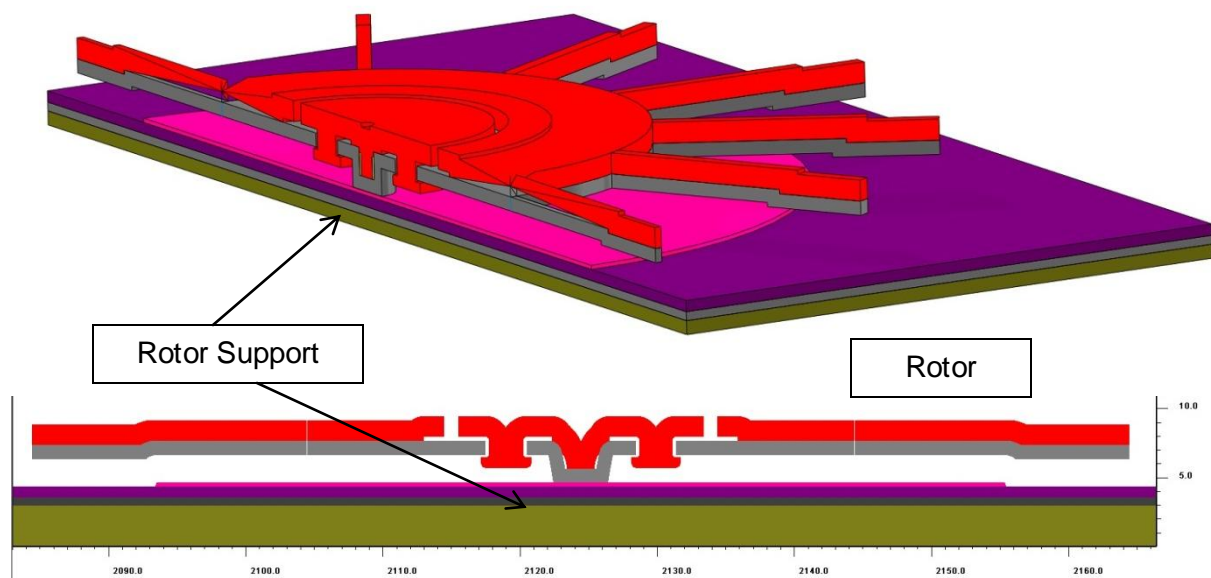


Figure 1.10: A 3D modeler view and cross-section model of a rotor created by gear generator.

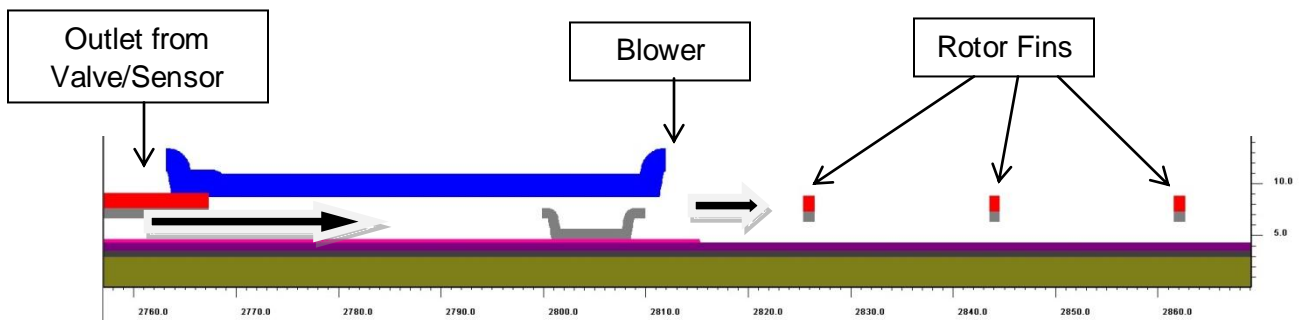


Figure 1.11: Cross-section model of final exit channel (blower) and rotor. Exit flow activate rotor with drag force.

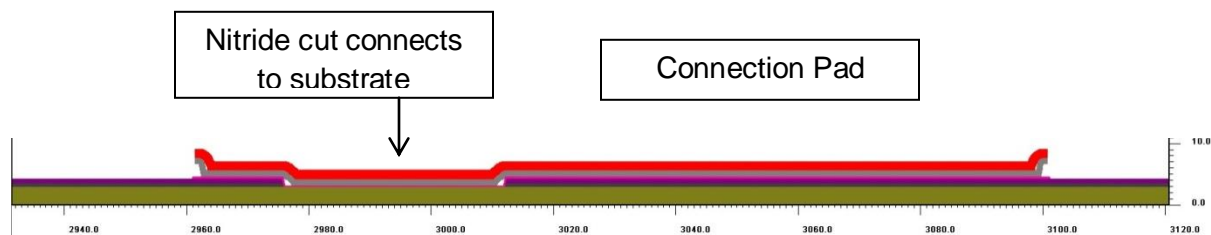


Figure 1.12: Cross-section model of electrical connection pad.

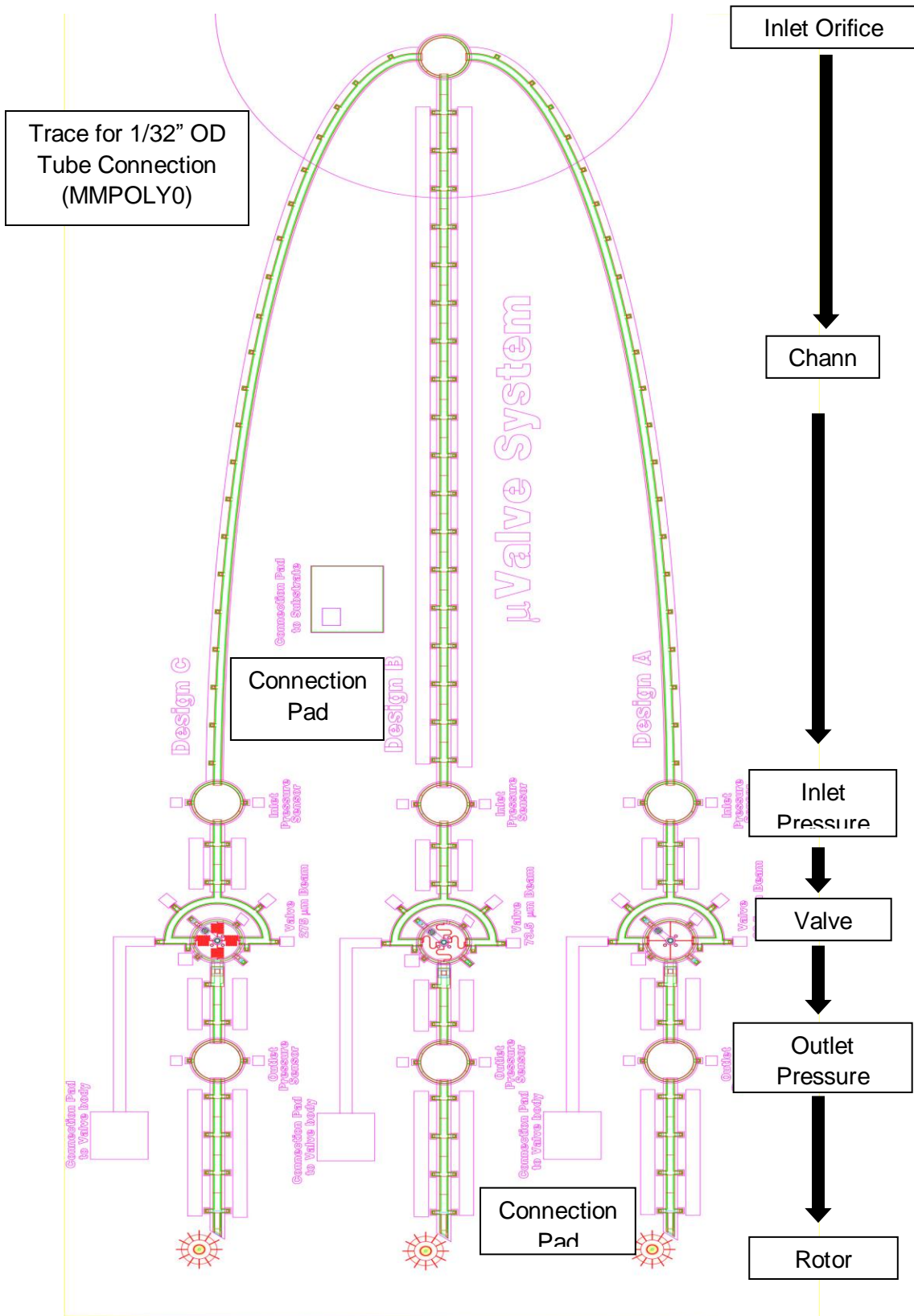


Figure 1.13: System Layout including three designs.

Appendix B: Test Setup Procedure

The following figure describes the experimental setup for the pressure-sensitive μ valve.

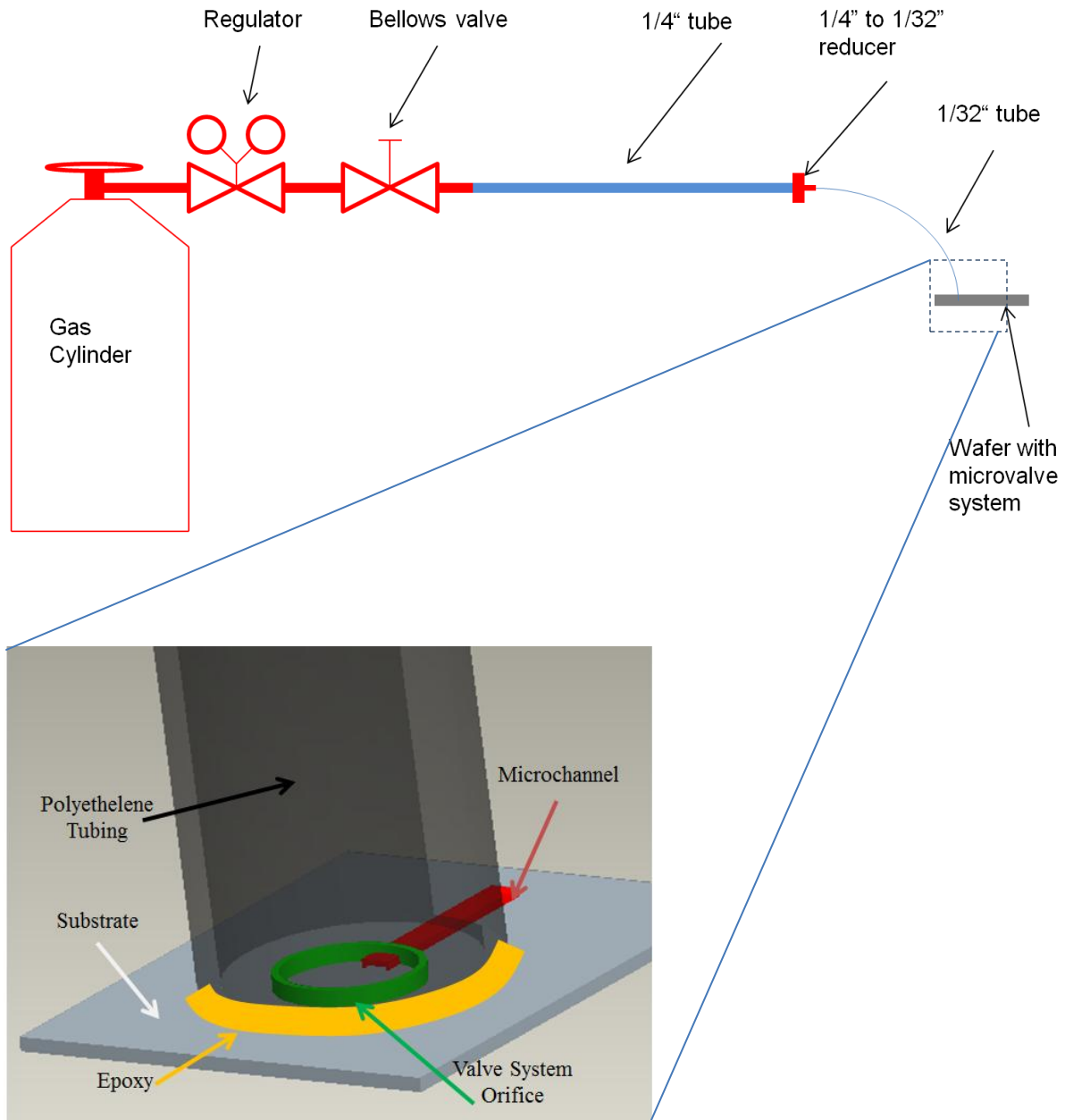


Figure 2: Test Procedure Setup. Supply of air flow is presented.

Appendix C: Parameter Descriptions

The following table lists all the parameters used throughout this report as well as a short description and a value if applicable. Figure 3. illustrates specific parameters

Table 1: Description of Parameters found in the report

| Parameter | Description | Values |
|----------------------|---|--------------------------|
| P | Pressure on the diaphragm in the pressure sensor | |
| P_{elec} | Electrostatic pressure exerted on the valve body | |
| $\delta_{diaphragm}$ | Deflection of the diaphragm in the pressure sensor | |
| δ_{nl} | Nonlinear deflection of valve beam | |
| δ_l | Linear deflection of valve beam | |
| δ | Total valve body deflection | |
| V | Applied Voltage | |
| F_{app} | Total applied force on valve body (fluidic & electrostatic) | |
| E | Young's Modulus | 164GPa |
| t | Thickness of diaphragm | 2.25 μ m |
| L | Length of valve beam | |
| I | Moment of Inertia of valve beam | .28 μ m ⁴ |
| ν | Poisson's Ratio | 0.28 |
| R | Diaphragm Radius | 40 μ m |
| ϵ_0 | Vacuum Permittivity | 8.85pF/m |
| D_e | Diameter of valve body affected by electrostatic force | 6.5 μ m |
| g | Gap distance between valve entry orifice and activation pad | 0.5 μ m |
| x | Valve body distance from the inner valve entry orifice | |
| u | Dummy variable used in nonlinear fixed-fixed beam calculation | |
| K_{eff} | Effective spring constant of valve beams | |

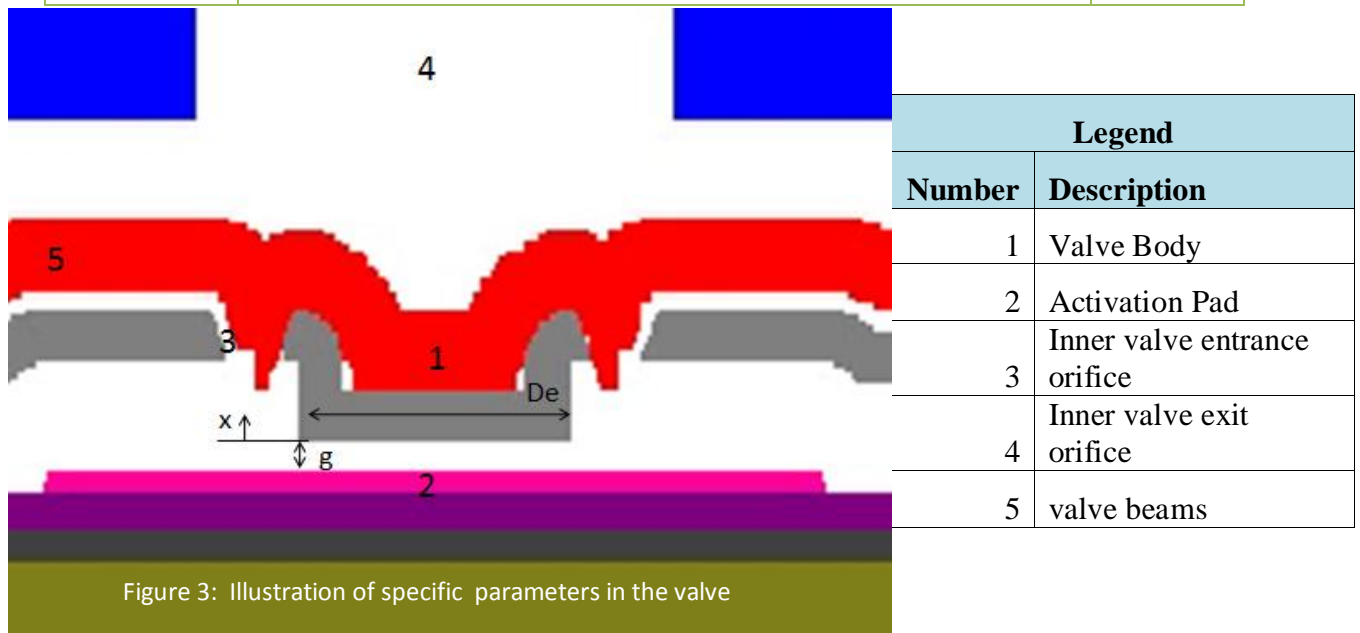


Figure 3: Illustration of specific parameters in the valve

Appendix D: Modeling Analysis – Pressure Sensor and Electrostatic Force Calculations

By utilizing equation 1, a graphical comparison between the pressure and the deflection of an 80 μm -diameter pressure sensor is developed and seen in Figure 4. This graph can be used to quickly convert deflection readings obtained from an interferometer to pressure readings to be used in other equations.

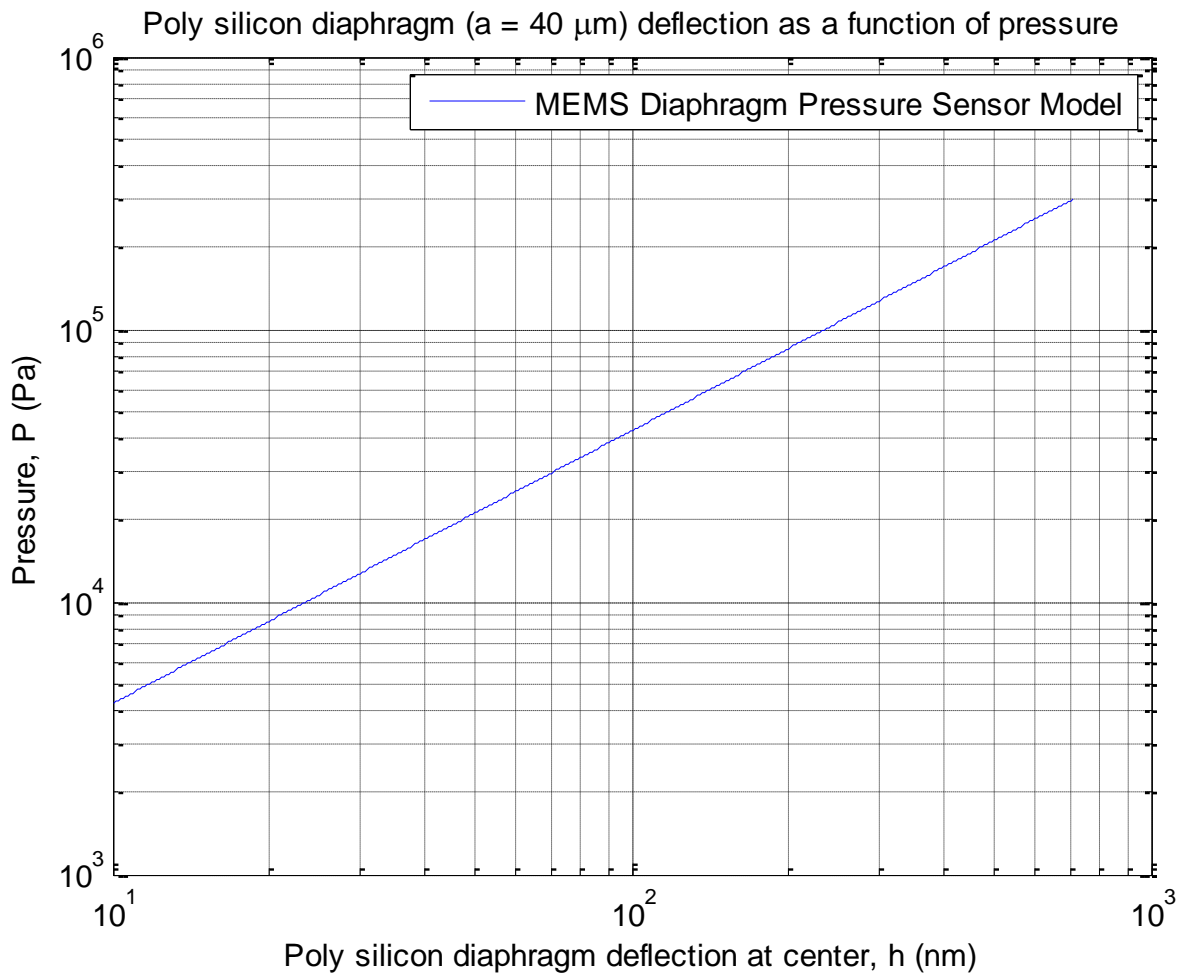


Figure 4: Deflection As a Function of Pressure for sensor as given by Equation 1

Figure 5 is a plot of the electrostatic force applied to the valve body occurring from a voltage applied to the system as calculated by equation 2. The three gap sizes (0.2 μm , 0.5, and 2.5) correspond to the three cases of our valve body covering the inner valve entrance orifice (valve closed), our valve body being in equilibrium (valve open), and our valve body covering the inner valve exit orifice (valve closed). From Figure 5, it is clear that the force is extremely large and difficult to overcome when the valve is initially closed, but once the valve opens, a much larger voltage must be applied to re-close the valve. Once the valve body is covering the inner valve exit orifice (gap of 2.5 μm), the electrostatic force has a negligible effect on the system.

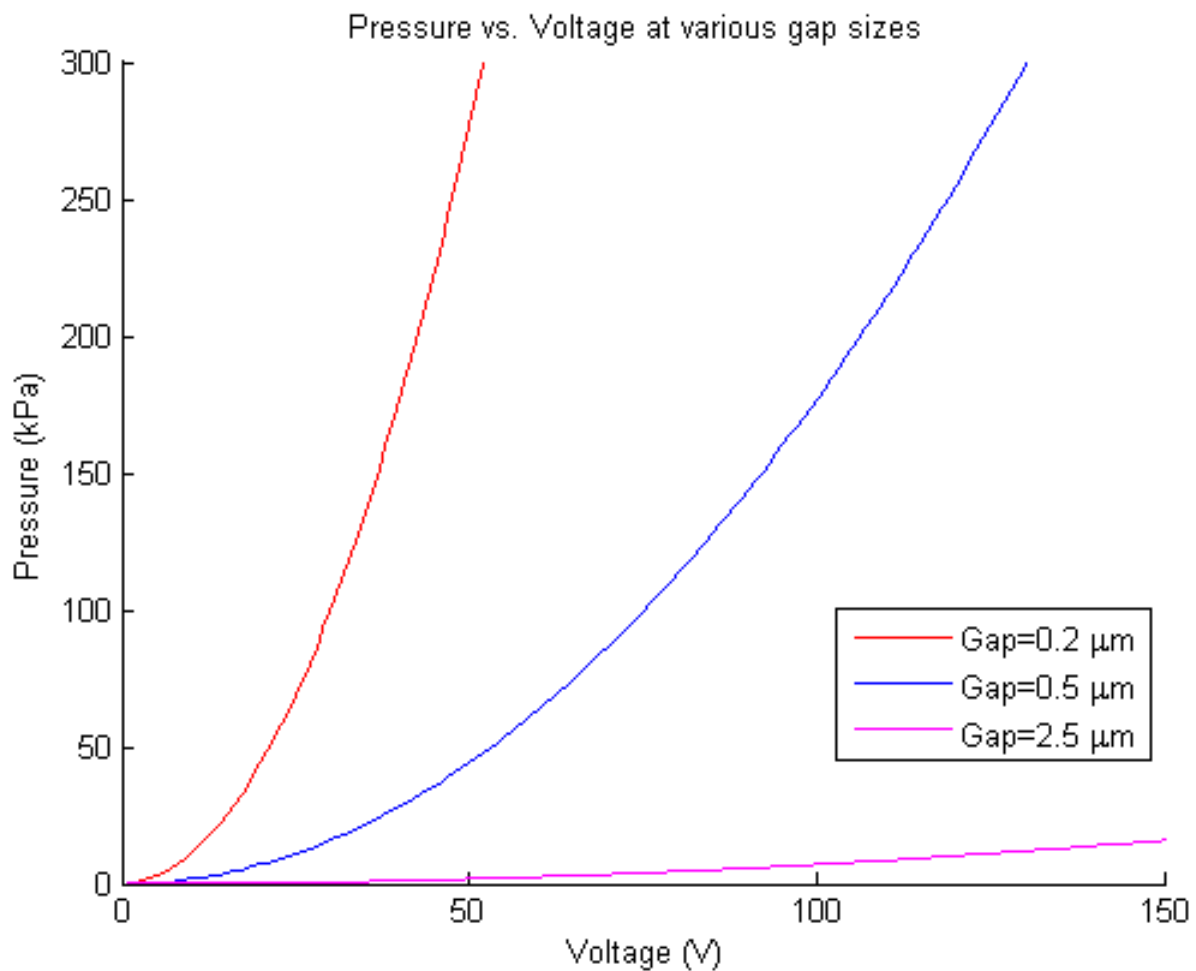


Figure 5: Electrostatic Pressure Exerted on Valve Body at Various Applied Voltages and Various Operational Stages

Appendix E: Modeling Analysis - Valve Beam Elasticity Analysis

In this appendix, the theoretical beam deflections are compared with an FEM model where the linear and nonlinear fixed-fixed beam deflection equations are taken to be equations 4 and 5 respectively [28]:

$$\delta_{nl} = \sqrt{\frac{2I}{A} \frac{(u - \tanh u)}{\frac{3}{2} - \frac{1}{2} \tanh^2 u - \frac{3 \tanh u}{2u}}} \quad \& \quad F_{app} = \frac{4EI}{L^2} \sqrt{\frac{2I}{A}} u^3 \frac{1}{\sqrt{\frac{3}{2} - \frac{1}{2} \tanh^2 u - \frac{3 \tanh u}{2u}}} \quad (\text{eqn 4})$$

$$\delta_L = \frac{F_{app} L}{192EI} \quad (\text{eqn 5})$$

The definitions and values of these variables are found in Table 1 in Appendix B. According to the law of linear superposition of beams, the total deflection is found by summing together the deflection due to each section of the beam independently. Therefore, the effective beam lengths found for each design are 32.5 μm , 73.5 μm , and 275 μm for designs A, B, and C respectively. For the FEM model, ABAQUS 6.9 FEM package was used to simulate the responses of all three designs due to an applied pressure of 100 kPa on the center 10 μm diameter of the valve body which would be affected (see Figures 6-8). The valve beams were fixed with displacement boundary conditions of zero. Design A gave a deflection of 0.053 μm , design B, which is more compliant due to the extended length of the beams, had a deflection of 0.393 μm and design C, the most compliant, deflected 1.013 μm . As seen in Figures 6-7, there is very good agreement between the linear, nonlinear, and FEM model for design A and mediocre agreement for design B. For design C however, neither the linear nor the nonlinear approximations are appropriate. As stated previously, this difference is due to the abnormal geometry of the beams.

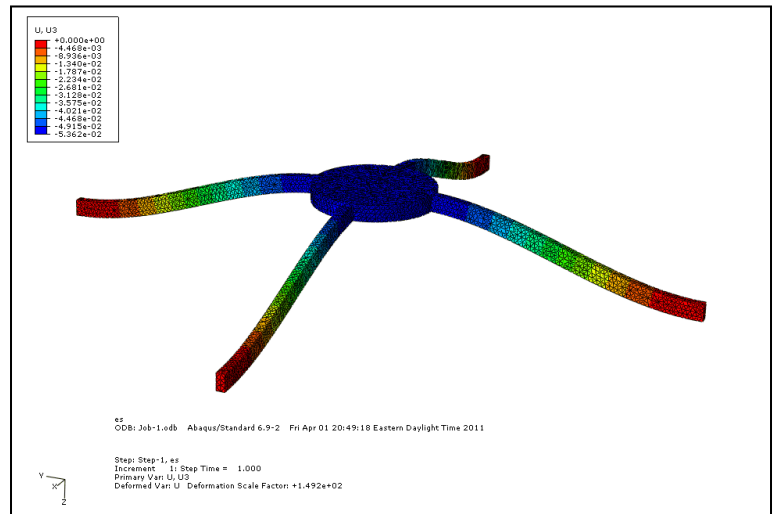
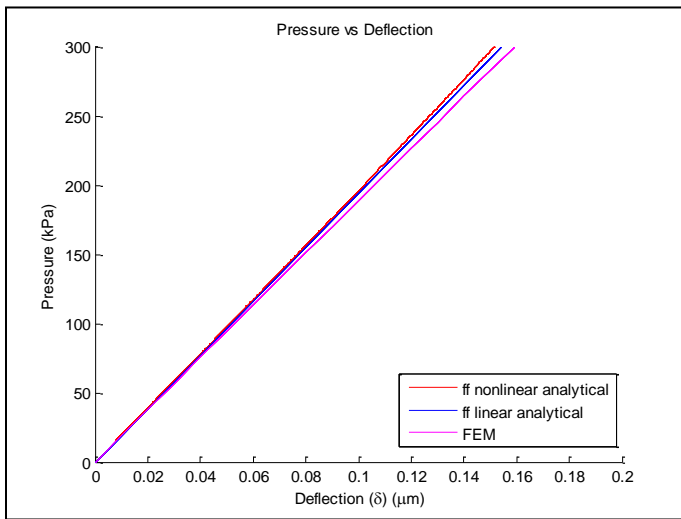


Figure 6: Left part includes design A deflection vs pressure plots with linear analytical calculation, nonlinear analytical calculation and FEM results. Right region shows deflected image at FEM simulation with 100 kPa

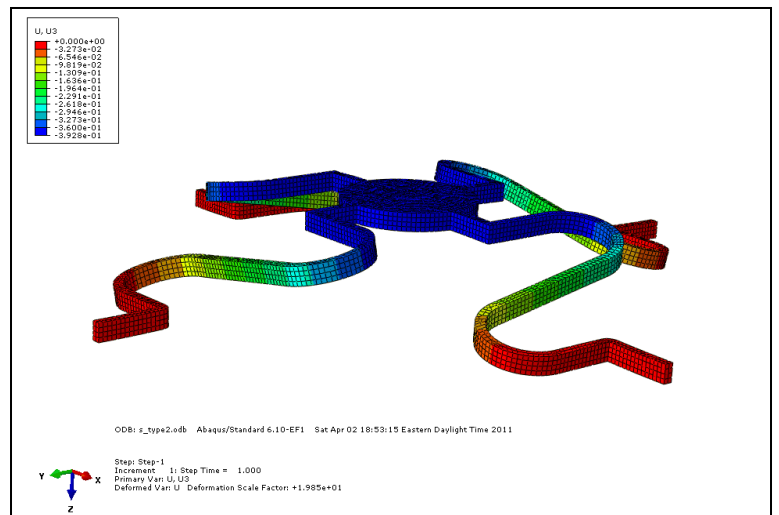
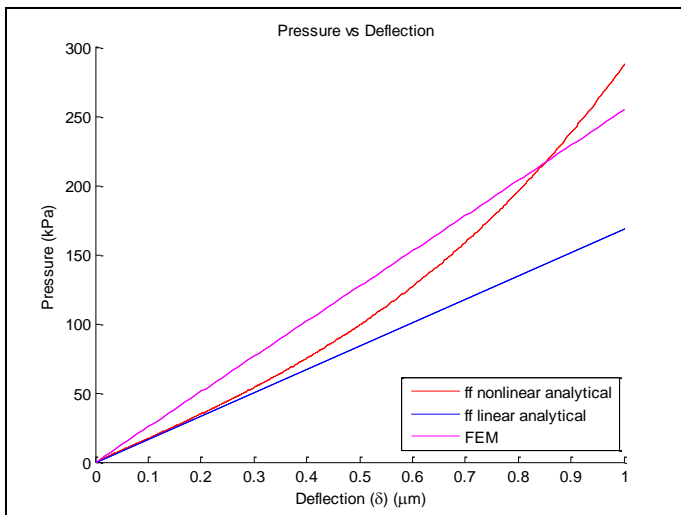


Figure 7: Left part includes design B deflection vs pressure plots with linear analytical calculation, nonlinear analytical calculation and FEM results. Right region shows deflected image at FEM simulation with 100 kPa.

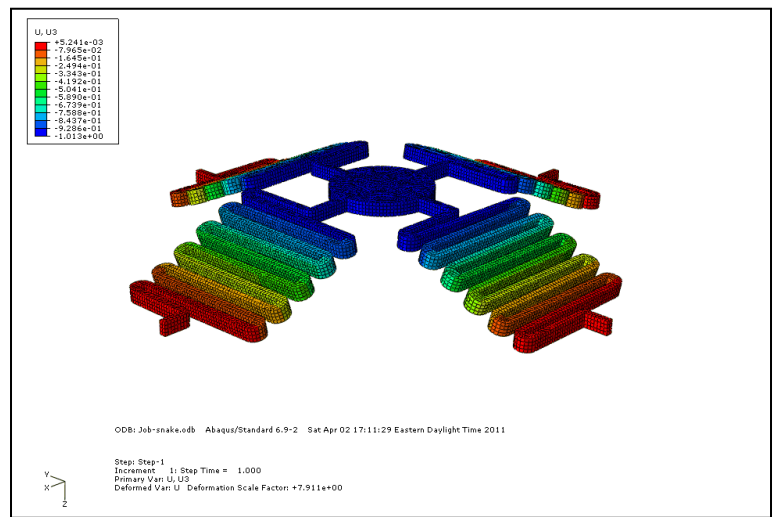
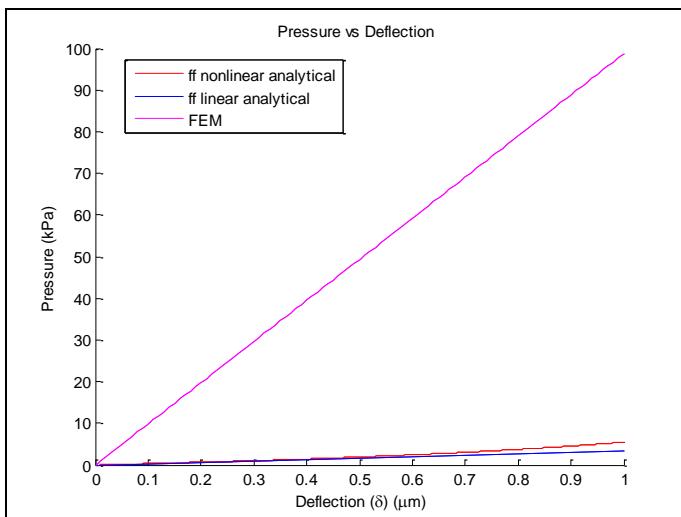


Figure 8: Left part includes design C deflection vs pressure plots with linear analytical calculation, nonlinear analytical calculation and FEM results. Right region shows deflected image at FEM simulation with 100 kPa.

Appendix F: Pressure Experiments Calculations

Test 2 – Opening Pressure Calculations

Convert the sensor deflection measurements to pressure readings as described in the modeling section. Since the opening pressure varies between systems, each of the valve assemblies is considered independently. When the valve is closed, no air flow passes through so the pressure sensor in the valve should read atmospheric pressure (100kPa). However, once the air pressure is large enough, the valve is forced open and the pressure sensor in the valve shows a dramatic increase and matches the inlet pressure reading since air is now flowing through. In summary, the opening pressure is the value of valve sensor's pressure reading once it first jumps above atmospheric.

This opening pressure is essential in calculating the compliance of the valve beams by determining the effective spring constant of the system. In the modeling section, equations 2-3 are used to relate the electrostatic force and the air pressure (found by the valve pressure sensor) to the mechanical properties of the system. Use these equations to determine the effective spring constant for all three systems. Notice how the effective spring constant differs between designs A, B, and C.

Test 3 – Closing Pressure Calculations

Convert the sensor deflection measurements to pressure readings using Figure 4 in appendix D as before. In the previous test, the compliance of each valve system was shown to be different so the closing pressure of each system is expected to vary between systems as well. When the valve is open, the air easily flows through the valve so the pressure of the inlet and the valve sensors are approximately the same. When the valve is forced closed due to the air pressure, the flow cannot pass through and the valve sensor should read a value close to atmospheric. This results in a dramatic pressure decrease (to approximately atmospheric) in the valve sensor at the closing pressure. The closing pressure is the value of the valve sensor's reading before it suddenly drops. If a drop in the pressure is not found, a possible cause is the valve being forced open due to particles getting trapped between the valve body and the exit orifice causing significant leakage or the valve beams are too stiff to close. Since the gap distance between the valve body and the exit plane is 2 μm , this can be used in conjunction with the spring constants for the three system that were determined in the last test to solve for the theoretical closing pressure by using equation 3. Compare the theoretical and experimental closing pressures for the three systems and note the difference in the closing pressures available between the systems.

Test 4 – Operational Pressure Range Calculations

The compliance of the system influences the size of the operation range; in a more compliant valve, the valve beams deflect under smaller loads and therefore close the valve under smaller pressures. This test only considers design B but theoretical values can be obtained for the other designs and checked experimentally. Convert the sensor deflection measurements to pressure readings using Figure 4 in Appendix D. As in the previous section, analyze the data to determine the opening and the closing pressure of this valve by finding the valve sensor's

pressure reading directly after it significantly increases (opening pressure) and directly before it significantly decreases (closing pressure). Compare this data with the theoretical values using the previously determined effective spring constant for this system and the values for the gap distances and the voltage in equation 2 and 3. The agreement between the two values will not be perfect due to the change in fluid flow due to varying gap distances as the valve body moves and the fact that the electrostatic gap changes as the valve body moves, but it will be accurate enough to be used as a rough estimate for determining the operational pressure range.

Test 5 – Leak Test

To inspect the reliability of the valve system, a leak test is performed. Initially, the idea for this test consisted of blocking the exit channel with epoxy, pressurizing the μ valve system to 200 kPa, and closing a macrovalve in the tubing. This, however, may not work because a comparatively large amount of air can leak through the valve in the tubing considering there is no clear way to verify that there is a hermetic seal in the macrovalve. Clamping the tube close to the wafer may improve this experiment, but also has the same problems. A suggestion is to submerge the system in deionized water, once the exit channel is blocked with epoxy, the tube is connected to the wafer, and 200 kPa is applied, and observe the creation of bubbles under a microscope. Furthermore, we will be able to identify the location of the leak and estimate the leak rate using a CCD camera. The system can be reused once the water has been evaporated.

Appendix G: Implementation of the rules (2011Categories.pdf document)

- 1) CMU is a participating member of the University Alliance Program.
- 2) CMU is submitting two modules.
- 3) The lead for this module in the Education Category is Vitali Brand.
- 4) Device is clearly marked using the construction layer.
- 5) The presubmission checklist and peer review were completed.
- 6) All designs pass the DRC.
- 7) All designs fit in the standard module size.
- 8) We would like to receive released modules to check functionality. No Aluminum bond pad is required for these designs.

Appendix H: References

- [1] Oh KW, Ahn CH; "A Review of μ valves," *Journal of μ mechanics and μ engineering*, Vol. **16**, 2006, R13-R394
- [2] Wang J, Manesh K; "Motion Control at the Nanoscale," *Small*, Vol. **6**, No. 3, 2010, 338-345
- [3] Medintz I, Paegel B, Mathies R; " μ fabricated Capillary Array Electrophoresis DNA Analysis Systems", *J. Chromatog. A*, 924, 2001, 265-270
- [4] Shikida M, Sato K, Tanaka S, Kawamura Y, Fujisaki Y; "Electrostatically driven gas valve with high conductance", *J. μ electromech. Syst.* **3**, 1994, 76-80
- [5] Goll C, Bacher W, Bustgens B, Maas D, Ruprecht R and Schomburg W K; "An electrostatically actuated polymer μ valve equipped with a movable membrane electrode," *J. μ mech. μ eng.* Vol. **7**, 224-6, 1997
- [6] Yoshida K, Tanaka S, Hagihara Y, Tomonari S, Esashi M; "Normally closed electrostatic μ valve with pressure balance mechanism for portable fuel cell application," *Sensors Actuators A*, **157**, 2009, 290-298
- [7] Yang X, Holke A, Jacobson S A, Lang J H, Schmidt M A, Umans S D; "An electrostatic, on/off μ valve designed for gas fuel delivery for the MIT μ engine," *J. μ electromech. Syst.*, Vol. **13**, 2004, 660-8
- [8] Schaible J, Vollmer J, Zengerle R, Sandmaier H, Strobel T; "Electrostatic μ valves in silicon with 2-way function for industrial applications," *11th Int. Conf. on Solid-State Sensors and Actuators (Transducers '01)*, 2001, 928-31
- [9] Messner S, Schaible J, Vollmer J, Sandmaier H, Zengerle R; "Electrostatic driven 3-way silicon μ valve for pneumatic applications," *μ electromech. Syst. Mems-03 Kyoto*, 2003, 88-91
- [10] Yobas L, Durand D M, Skebe G G, Lisy F J, Huff M A; "A novel integrable μ valve for refreshable Braille display system" *J. μ electromech. Syst.* **12**, 2003, 252-63
- [11] Yobas L, Huff M A, Lisy F J, Durand D M; "A novel bulk μ machined electrostatic μ valve with a curved-compliant structure applicable for a pneumatic tactile display," *J. μ electromech. Syst.*, **10**, 2001, 187-96
- [12] Mastrangelo C H; "Thermal applications of μ bridges" *PhD Thesis* University of California at Berkeley, 1991
- [13] Eaton WP, Smith JH; " μ machined pressure sensors: review and recent developments," *Smart Mater. Struct.*, 1997, pg 530-539
- [14] Timoshenko S, Woinosky-Krieger S; *Theory of Plates and Shells*, 1987
- [15] Smith C S; "Piezoresistance effect in germanium and silicon," *Phys. Rev.* **94**, 1954, 42-9
- [16] Bryzek J, Petersen K, Mallon J R, Christel L, Pourahmadi F; *Silicon Sensors and μ structures*, 1990
- [17] Cho S T, Najafi K, Wise K D; "Secondary sensitivities and stability of ultrasensitive silicon pressure sensors," *Tech. Digest 1990 IEEE Solid-State Sensor and Actuator Workshop (Hilton Head, SC, 1990)*, 1990
- [18] Sch'oenberg U, Schnatz F V, Brockherde W; "CMOS integrated capacitive pressure transducer with on-chip electronics and digital calibration capability," *Digest Tech. Papers 1991 Int. Conf. on Solid-State Sensors and Actuators (Transducers '91)*, 1991, p 304
- [19] Schnatz F V, Sch'oenberg U, Brockherde W, Kopystynski, Mehlorn T, Obermier E, Benzel H; "Smart CMOS capacitive pressure transducer with on chip calibration capability," *Sensors Actuators A*, **34**, 1992, 77-83
- [20] Wagner D, Frankenberger J, Deimel P; "Optical pressure sensor using two Mach-Zehnder interferometers for the TE and TM polarizations," *J. μ mech. μ eng.* **4**, 1994, 35-9
- [21] Dzuiban J A, Gorecka-Drzazga A, Lipowicz U; "Silicon optical pressure sensor," *Sensors Actuators A*, **32**, 1992, 628-31
- [22] Hoppe K, Anderson L U A, Bouwstra S; "Integrated Mach-Zehnder interferometer pressure transducer," *8th Int. Conf. on Solid-State Sensors and Actuators (Transducers '95)*, 1995, pp 590-5
- [23] Chan M A, Collins S D, Smith R L; "A μ machined pressure sensor with fiber-optic interferometric readout," *Sensors Actuators A*, **43**, 1994
- [24] Galambos P, Eaton W, Shul R, Willison C, Sniegowski J, Miller S, Gutierrez D; "Surface μ machine μ fluidics: Design, Fabrication, Packaging, and Characterization", Sandia National Labs, 1999
- [25] Jensen BD, de Boer MP, Masters ND, Bitsie F, and LaVan DA, "Interferometry of actuated cantilevers to determine material properties and test structure nonidealities in MEMS," *J. μ electromech. Syst.*, vol. **10**, p. 336, 20
- [26] Timoshenko S, Goodler, J; *Theory of Elasticity Third Edition*, McGraw-Hill, 1970
- [27] Liao E. B., Tay A. A. O., Ang S. S. T., Feng H. H., Nagarajan R., Kripesh V., Kumar R. and Iyer M.K. A MEMS-Based compliant interconnect for ultra-fine-pitch wafer level packaging *Electronic Components and Technology Conference, 2006. Proceedings. 56th* 1246-1250
- [28] Frish-Fay R; "Flexible Bars," Butterworths Scientific Publications, 1963, 83-91
- [29] Whiting, J, Roukes M, Myers E, McBrady A, Friedhoff, C; "Fieldable Micro Gas Analyzers," <http://www.cpac.washington.edu/Activities/Meetings/Fall/2010/documents/SimonsonCPACv3.pdf>, 4/5/2011
- [30] IEEE Transactions on Education and Journal of Engineering Education
- [31] ASEE (American Society for Engineering Education)